Journal of Cellular Biochemistry 90:361–378 (2003)

A Proteomic Study of the Arabidopsis Nuclear Matrix

Tomasz T. Calikowski,[1,3] Tea Meulia,[2] and Iris Meier[1]*

[1]Department of Plant Biology and Plant Biotechnology Center, Ohio State University, Columbus, Ohio 43210
[2]Molecular and Cellular Imaging Center, Ohio Agricultural and Research Development Center, Ohio State University, Columbus, Ohio 43210
[3]Institute of Biochemistry and Biophysics, Polish Academy of Sciences, UL. Pawinskiego, 5A, 02-106, Warszawa, Poland

Abstract The eukaryotic nucleus has been proposed to be organized by two interdependent nucleoprotein structures, the DNA-based chromatin and the RNA-dependent nuclear matrix. The functional composition and molecular organization of the second component have not yet been resolved. Here, we describe the isolation of the nuclear matrix from the model plant Arabidopsis, its initial characterization by confocal and electron microscopy, and the identification of 36 proteins by mass spectrometry. Electron microscopy of resinless samples confirmed a structure very similar to that described for the animal nuclear matrix. Two-dimensional gel electrophoresis resolved approximately 300 protein spots. Proteins were identified in batches by ESI tandem mass spectrometry after resolution by 1D SDS–PAGE. Among the identified proteins were a number of demonstrated or predicted Arabidopsis homologs of nucleolar proteins such as IMP4, Nop56, Nop58, fibrillarins, nucleolin, as well as ribosomal components and a putative histone deacetylase. Others included homologs of eEF-1, HSP/HSC70, and DnaJ, which have also been identified in the nucleolus or nuclear matrix of human cells, as well as a number of novel proteins with unknown function. This study is the first proteomic approach towards the characterization of a higher plant nuclear matrix. It demonstrates the striking similarities both in structure and protein composition of the operationally defined nuclear matrix across kingdoms whose unicellular ancestors have separated more than one billion years ago. J. Cell. Biochem. 90: 361–378, 2003.

Key words: nuclear matrix; nucleolus; arabidopsis; proteomics; mass spectrometry

One of the principal features of eukaryotic organisms is the presence of the nucleus, the subcellular compartment containing the genetic material. The architecture of the nucleus is thought to be composed of two mutually interrelated structures, both containing nucleic acids: chromatin and a nuclear matrix [van Holde, 1989; Hancock, 2000; Nickerson, 2001]. The latter one is envisioned to function as a karyoskeletal, non-histone structure that serves as a support for the genome and its activities, based on early electron microscopic studies, performed on unextracted cells [Fawcet, 1966]. Other early electron microscopic studies [Smetana et al., 1966] have shown that an important role in the ultrastructure and composition of the nuclear matrix, described as a proteinaceous skeleton in the nucleus, is played by the ribonucleoprotein (RNP) network [Nickerson, 2001].

It has been proposed that nuclear matrices generally consist of a nuclear lamina and pore complexes surrounding an internal fibrogranular network of RNP proteins and residual nucleoli [Penman, 1995]. An important feature of a nuclear matrix, demonstrated first by Berezney and Coffey [1974], is its resistance to DNase digestion, and insolubility upon extraction of isolated nuclei with detergents and high ionic strength buffers [Berezney and Coffey, 1977]. Since these early studies, which formulated the nuclear matrix' role as a critical

Grant sponsor: National Science Foundation, Ohio State University Plant-Microbe Genomics Facility (Proteomics Seed Grant).

*Correspondence to: Iris Meier, Department of Plant Biology and Plant Biotechnology Center, Ohio State University, 244 Rightmire Hall, 1060 Carmack Rd., Columbus, OH 43210. E-mail: meier.56@osu.edu

Received 28 May 2003; Accepted 24 June 2003

DOI 10.1002/jcb.10624

key factor facilitating DNA replication, RNA processing, RNA transport, among other functions [reviewed in Berezney et al., 1995], the current views on the topic have become more cautious [Hancock, 2000; Martelli et al., 2002] or even skeptical [Pederson, 1998; Pederson, 2000].

For example, RNA-bound proteins can undergo unexpected rearrangements when dislodged from their usual RNA associations, and once released, can spontaneously form filaments [Lothstein et al., 1985; Tan et al., 2000]. Furthermore, the various preparation methods used to extract nuclear matrix may result in non-physiological aggregation and precipitation, even on the initial step of isolation of nuclei or during their stabilization (reviewed recently by Pederson [2000]). The more extensive our body of knowledge about the proteins that make up the nuclear matrix, the easier it should become to elucidate its potential role in nuclear organization and to address if—and which—in vivo protein–protein interactions are responsible for its formation.

The rapidly evolving field of mass spectrometry-based proteomic investigation allows for the identification of novel proteins, and for the evaluation of roles of known functional components in different cellular compartments or the whole organisms [e.g., Washburn et al., 2001]. Recent proteomic studies of subnuclear compartments included the mouse nuclear envelope [Dreger et al., 2001] and the human nucleolus [Andersen et al., 2002; Scherl et al., 2002]. A comparative proteomic approach has been used to investigate the apoptosis-related changes in the structure of nuclear matrix of cultured cancer cells [Gerner et al., 2002].

Here, we report the first ultrastructural and proteomic characterization of the nuclear matrix of the model flowering plant Arabidopsis. Resinless electron microscopy revealed a striking similarity of the material isolated from Arabidopsis suspension culture cells with the well-documented animal nuclear matrix. Identification of 36 proteins by mass spectrometry demonstrated that several classes of functional proteins in the nuclear matrix are shared between vertebrates and higher plants. In addition, a number of novel proteins were identified. Together, they can now form the basis of a more comprehensive investigation of in vivo protein–protein interactions of the proteins co-isolated from a nuclear matrix fraction.

MATERIALS AND METHODS

Plant Cell Culture Growth and Maintenance

Arabidopsis suspension-cultured cells were grown in 50 ml of Gamborg B5 medium (Sigma, St. Louis, MO) supplemented with 1.1 mg/L 2,4-D and 0.5 g/L MES at 22°C under continuous fluorescent white light (60 μmol $m^2 \cdot s^1$). Cells were subcultured every 7 days at a 10-fold dilution with fresh medium.

Isolation of Nuclei and Nuclear Matrices

Arabidopsis nuclei and nuclear matrices (NM) were isolated essentially as described [Hall et al., 1991], except that the halos were digested with RNase-free DNaseI (GibcoBRL, Rockville, MD) instead of restriction enzymes. For 1D SDS–PAGE, NM aliquots were centrifuged and the pellets resuspended in sample solubilization buffer (2% SDS, 50 mM Tris, pH 7.6; 30% glycerol) and boiled for 10 min. Protein gels were stained with Coomassie Brilliant Blue R-250 stain (Sigma).

Immunoblot Analysis

Immunoblots were performed essentially as described [Gindullis and Meier, 1999; Rose et al., 2003]. A dilution of 1:3,000 of anti-LeNMP1 and of 1:10,000 for horseradish peroxidase-coupled donkey anti-rabbit secondary antibody were used, and detection was performed by the enhanced chemiluminescent method as described by the manufacturer (Amersham Biosciences, Piscataway, NJ).

Two-Dimensional Gel Electrophoresis

For two-dimensional (2D) electrophoresis, 10 nM aliquots were pooled (equal to 1 nuclear aliquot, approximately 75 μg of protein), centrifuged, and the pellet was washed once with water, followed by the primary solubilization in SDS-sample buffer (2% SDS, 50 mM Tris, pH 7.6) at 100°C for 5 min. A trichloroacetic acid precipitation (10% trichloroacetic acid in acetone) at −20°C for 1.5 h was followed by two 100% acetone washes, air-drying and resolubilization in 2D urea buffer (7 M urea, 2 M thiourea, 2% (w/v) CHAPS (Sigma), 2% (w/v) SB3–10 (Sigma), 0.2% (v/v) amphylites 3–10 (BioRad, Hercules, CA), 0.5 mM β-mercaptoethanol) for 1 h at 30°C. The supernatant was saved, and the pellet was resolubilized again with the same buffer for 15 min at 37°C. Both supernatants were pooled in the final volume of 100 μl. The

first dimension was run on a Protean IEF Cell (350 V for loading, 2.5 h of a linear ramp to 8,000 V, focusing for 30,000 V·h at 8,000 V). The second dimension was resolved in a Criterion Cell (BioRad) with running buffer 1 × TGS, at 200 V for 1 h (200 V·h total run). Gels were stained with SyproRuby (for visualization of faint spots), or Coomassie Brilliant Blue (for coring spots for mass spectrometry).

Protein Digestion

For the in-gel trypsin digestion of proteins excised as Coomassie-stained bands from the 1D-SDS polyacrylamide gels, and as spots from the 2D-SDS polyacrylamide gels, the Montage In-Gel Digest$_{96}$ Kit from Millipore was used.

MALDI–TOF and ESI–MS/MS Mass Spectrometric Methods

MALDI–TOF/MS. Matrix-assisted laser desorption/ionization time-of-flight (MALDI–TOF) was performed on a Bruker Reflex III (Bruker, Bremen, Germany) mass spectrometer operated in linear, positive ion mode with a N2 laser. Laser power was used at the threshold level required to generate signal. Accelerating voltage was set to 28 kV. The instrument was calibrated with protein standards bracketing the molecular weights of the protein samples (typically mixtures of bradykinin fragment 1–5 and ACTH fragment 18–39 as appropriate). Salt buffers from the protein samples were cleaned using ZipTips (Millipore, Bedford, MA) according to manufacturer's directions. α-cyano-4-hydroxy-cinamic acid was used as the matrix and prepared as a saturated solution in 50% ACN/0.1% TFA (in water). Allotments of 1 μl of matrix and 1 μl of sample were thoroughly mixed together; 0.5 μl of this mixture was spotted on the target plate and allowed to dry. A mass list of peptides was obtained for each protein digest. Next, the peptide mass fingerprint was submitted to ProFound (http://prowl.rockefeller.edu/cgi-bin/ProFound) to identify proteins.

Nano-LC MS/MS. Capillary-liquid chromatography-nanospray tandem mass spectrometry (Nano-LC/MS/MS) were performed on a Micromass in a hybrid quadrupole time-of-flight Q-Tof(tm) II (Micromass, Wythenshawe, UK) mass spectrometer equipped with an orthogonal nanospray source from New Objective, Inc. (Woburn, MA) operated in a positive ion mode. The LC system was a Waters Alliance 2690 Separation Module (Waters, Milford, MA). The solvent A was water containing 50 mM acetic acid and the solvent B was acetonitrile. Ten microliters of each sample was first injected on to the trapping column, and then washed with 50 mM acetic acid. The injector port was switched to inject and the peptides were eluted off of the trap onto the column. A 10 cm 50 mM ID BioBasic C18 column packed directly in the nanospray tip was used for chromatographic separations. Peptides were eluted directly off the column into the Q-TOF system using a gradient of 3–80% B over 20 min, with a flow rate of 280 ml/min with a pre-column split to about 500 ml/min. A total run time was 35 min. The nanospray capillary voltage was set at 2.8 kV and cone at 55 V. The source temperature was maintained at 100°C. Mass spectra were recorded using MassLynx 3.5 automatic switching functions. Mass spectra were acquired from mass 300–2,000 Da/s with a resolution of 8,000 (FWHM). When the desired peak (using include tables) was detected at a minimum of 8 ion counts, the mass spectrometer automatically switched to acquire CID MS/MS spectrum of the individual peptide. Collision energy was set dependent on charge state recognition properties. Sequence information from the MS/MS data was processed using the MassLynx 3.5 Biolynx software. Amino acid sequences, sequence tags and peptide ion fragments were used to screen the protein databases with MASCOT (http://www.matrixscience.com/cgi/index.pl?page = ../home.html), SONAR MS/MS (http://65.219.84.5/service/prowl/sonar. html), BLAST (http://www.ncbi.nlm.nih.gov/ BLAST/) [Altschul et al., 1990], or FASTA3 (http://www.ebi.ac.uk/fasta3).

Epifluorescent and Confocal Microscopy

For inverted epifluorescent microscopy (Leica DM IRB), material was stained for 5 min with 300 nM 4′,6′-diamidino-2-phenylindole hydrochloride (DAPI) in 0.1 M potassium phosphate buffer (pH 7.4). Images were taken with the Optronics Magnafire digital camera (image size 1300 × 1030 pixels; pixel size 6.7 × 6.7 μm) with a UV filter A BP340-380/400/LP425.

For confocal microscopy, the samples were stained for 5 min with 500 nM propidium iodide (PI) in 0.1 M potassium phosphate buffer (pH 7.4), to visualize nucleic acids. The PI images were taken on the Leica TCS SP scanning confocal microscope using the Argon laser

(488 nm) for the excitation, and detection was performed at 610–640 nm.

Preparation of DGD Resinless Sections

Resinless nuclear matrix sections were obtained essentially as described [Nickerson et al., 1990; Yu and Moreno Diaz de la Espina, 1999]. Briefly, nuclear matrices were fixed in 2.5% glutaraldehyde in 0.1 M potassium phosphate buffer (pH 7.4) for 1 h at RT, rinsed three times with phosphate buffer and then embedded in 0.8% low melting agarose. Samples were post-fixed in 1% OsO_4 for 30 min at room temperature, dehydrated through an ethanol and n-butyl alcohol series and embedded in diethylene glycol distearate (DGD). Sections (500 nm) were collected on Formovar-carbon coated, and poly-L-lysine treated grids. DGD was removed by treating the grids with 100% n-butyl alcohol, 50% n-butyl and 50% ethanol, and two changes of 100% ethanol. Grids were then critically point dried and observed using a Hitachi N7500 electron microscope at 80 or 60 kV.

Computational Methods

For prediction of subcellular localization, ProtComp 4 (Softberry, Inc., Mount Kisco, NY; http://www.softberry.com/berry.phtml?topic=proteinloc), PSORT v.6.4, (http://psort.nibb.ac.jp/form.html) [Nakai and Kanehisa, 1992)], and PredictNLS (http://cubic.bioc.columbia.edu/predictNLS) [Cokol et al., 2000] were used. The calculation of theoretical pI values was performed with EXPASY (http://us.expasy.org/tools/pi_tool.html), and the coiled-coil prediction with the Protein Analysis module of the LASERGENE package (DNAX Corp.).

RESULTS

Isolation of the Arabidopsis Nuclear Matrix and Its Initial Characterization

To isolate the nuclear matrix fraction from Arabidopsis suspension culture cells, we adopted the protocol of Mirkovitch et al. [1984], modified later for tobacco cells [Hall et al., 1991]. This protocol exploits the lithium 3,5-diiodosalycylate and digitonin extraction of chromatin proteins. Its main advantage over high-salt extraction of chromatin proteins is a lower risk of artifactual NaCl-induced precipitation of nuclear proteins [Pederson, 2000]. However, the ultrastructures revealed by both methods show a marked similarity in the underlying network of branched 10 nm filaments [Nickerson, 2001].

The isolation procedure was monitored by brightfield and fluorescent microscopy (Fig. 1). Propidium iodide (PI) staining was used to monitor the presence of nucleic acids and DAPI staining to distinguish between DNA and RNA. Nuclear matrices showed significant reduction of DAPI fluorescence (Fig. 1K,L), indicating the successful removal of genomic DNA. The remaining propidium iodide fluorescence was concentrated in the nucleolar matrix (Fig. 1I,J), likely corresponding to RNA.

Resinless section electron microscopy was used to determine the ultrastructural appearance of the material (Fig. 2). The structures showed a network of fibers, well distributed through the entire body of the nuclear matrix, and connected to the nucleolar matrix. At higher magnification (Fig. 2B) the fibers of the nuclear matrix appear of different diameter, and are covered in multiple protrusions ("knobby" appearance, arrows). In a number of regions a more dense fibrillonuclear network can be seen (Fig. 2C, pointed bracket), intermixed with regions of a more loose organization (Fig. 2C, blunt bracket). Together, the ultrastructure of the isolated Arabidopsis nuclear matrix closely resembles that described from other organisms [Belgrader et al., 1991; Nickerson et al., 1997; Yu and Moreno Diaz de la Espina, 1999].

The protein profile of the Arabidopsis nuclear matrix was compared to whole nuclei by 1D SDS–PAGE (Fig. 3A). The bands corresponding to the core histones and histone H1 are absent from the nuclear matrix fraction, indicating the proper extraction of soluble and chromatin-bound proteins. Most nuclear matrix proteins appear in the size range from 20 to 100 kDa. An antiserum against a nuclear matrix-associated protein from tomato (LeNMP1) [Rose et al., 2003] detects a single protein of the expected size 36 kDa, which is retained in the nuclear matrix fraction (Fig. 3B). As a negative control to eliminate the possibility of contamination, we used an antiserum against α-sulfite reductase, a protein located in chloroplasts [Chi-Ham et al., 2002]. Even though it detected a protein of the correct size (70 kDa) in both the *Arabidopsis* whole cell extract and a chloroplast preparation, it did not detect this protein in both nuclei and the nuclear matrix fraction (results not shown).

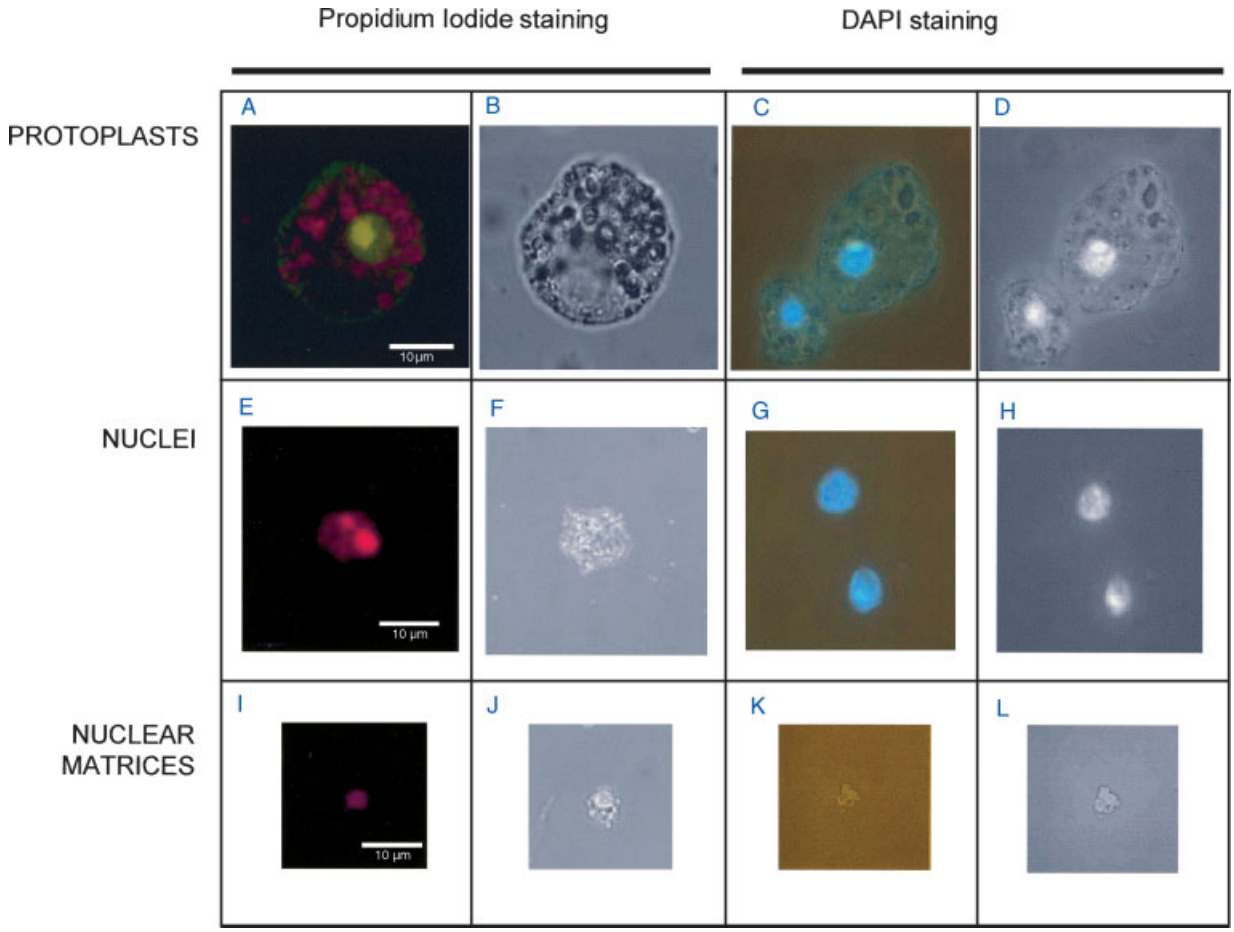

Fig. 1. Visual inspection of the nuclear matrix isolation procedure. **A–D**: Arabidopsis protoplasts; (**E–H**) nuclei; (**I–L**) nuclear matrices; (A, E, I) propidium iodide staining (A: green, propidium iodide; red, chloroplast autofluorescence; E, I: propidium iodide); (D, H, L) DAPI staining; (B, F, J) bright field images; (C, G, K) composite bright field and fluorescent images after DAPI staining.

Resolution of the Nuclear Matrix by 2D-PAGE

The nuclear matrix is, by definition, highly insoluble. We developed a solubilization protocol compatible with isoelectric focussing (see "Materials and Methods") and resolved a sample by 2D-PAGE (Fig. 4). In total, 365 individual spots could be identified after image enhancement with the PDQuest computer program (BioRad, Hercules, CA, Fig. 4C), confirming the expected complexity of this nuclear fraction. The most abundant proteins were found predominantly in the range of pI 4.8–pI 7.5, and of 20–100 kDa, as shown in the insets in Figure 4B. Figure 4D shows an immunoblot with the anti-LeNMP1 antibody, confirming the presence of this protein in the analyzed fraction. After detection, a stronger signal likely to correspond to the main protein isoform and a weaker signal shifted towards the basic region of the gel could be seen. Because tomato NMP1 was shown to contain six predicted protein kinase CKII phosphorylation sites [Rose et al., 2003], it is possible that this electrophoretic behavior indicates the existence of phosphorylated variants of this protein within the context of the *A. thaliana* nuclear matrix. Additional experiments might pinpoint the actual sites for phosphorylation and the kinase responsible for this potential activity.

Three of the most abundant protein spots were selected for coring from a corresponding Coomassie-stained 2D gel (spots C1, D2, and F2 in Fig. 4B,C), resulting in the identification of five proteins (Table I).

Tandem Mass Spectrometry of Proteins Isolated From 1D SDS–PAGE Regions

Because identification of proteins from 2D-PAGE is biased towards soluble proteins,

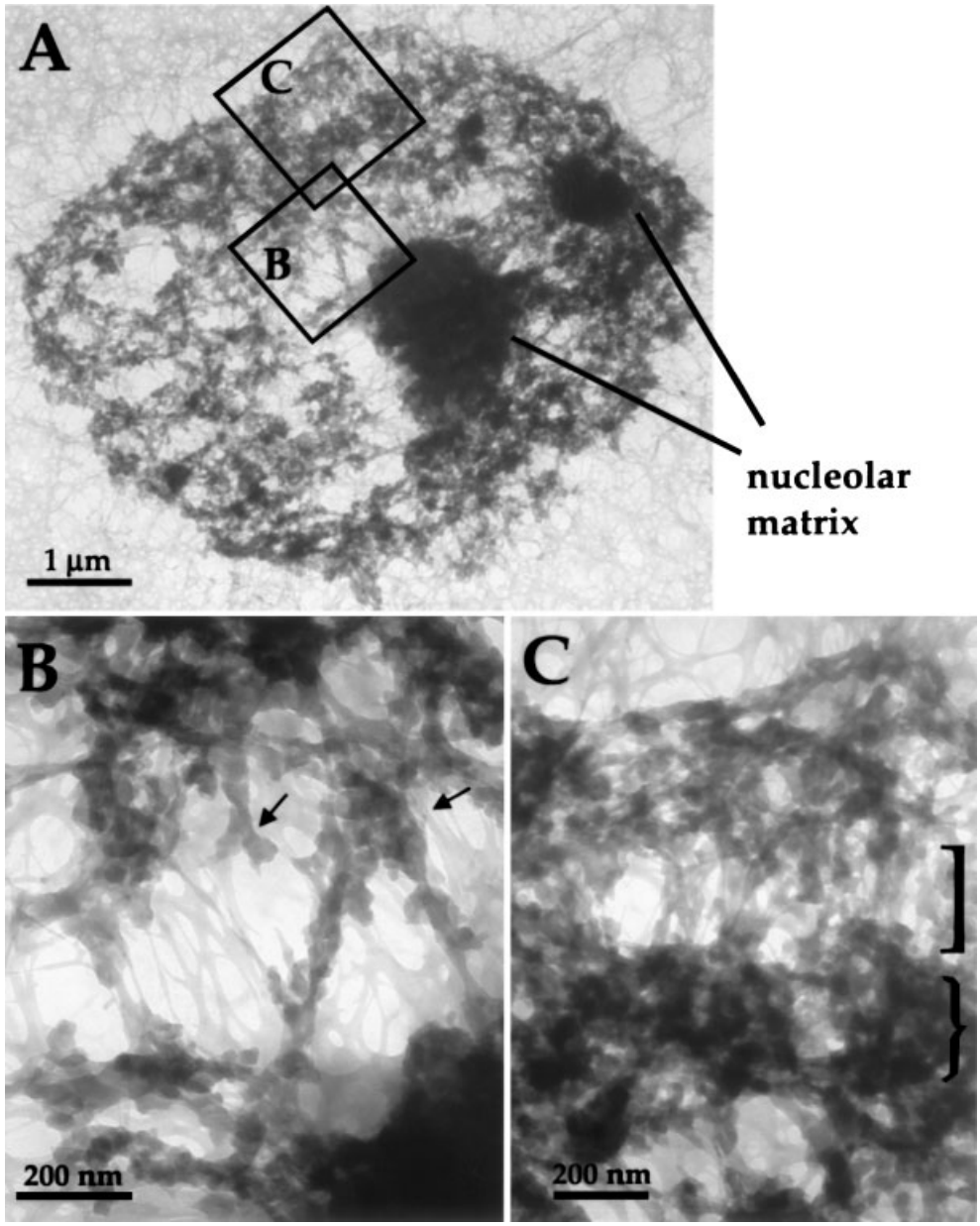

Fig. 2. Ultrastructural analysis of the Arabidopsis nuclear matrix (resinless preparations), as observed under the transmission electron microscope. The nucleolar matrix is indicated in (**A**). **B**, **C**: higher magnification images corresponding to areas labeled B and C in (A). Note the multiple branching sites within the nucleofibrillar network (arrows in B) and ''knobby'' appearance of the fibers of the nuclear matrix, with dense regions (pointed bracket), and regions of a more loose structure (blunt bracket) in (C).

samples for protein identification were instead resolved on 1D SDS–polyacrylamide gels. The gels were stained with Coomassie blue, and seven sections were excised (Fig. 3B) and submitted for electrospray-ionization tandem mass spectrometry (ESI–MS/MS) analysis. This analysis was repeated two to four times per gel section.

Data obtained by ESI–MS/MS were analyzed with Mascot or Sonar software and hits with a significant Mascot (Mowse) or Sonar score are listed in Table II. The number of peptides identified for each protein varied between 1 and 16. For proteins with a single peptide hit, the run was repeated with a different nuclear matrix sample, but the same peptide was found in the second MS/MS analysis.

We analyzed the predicted subcellular localization of the proteins listed in Table I and II by using a number of protein-localization

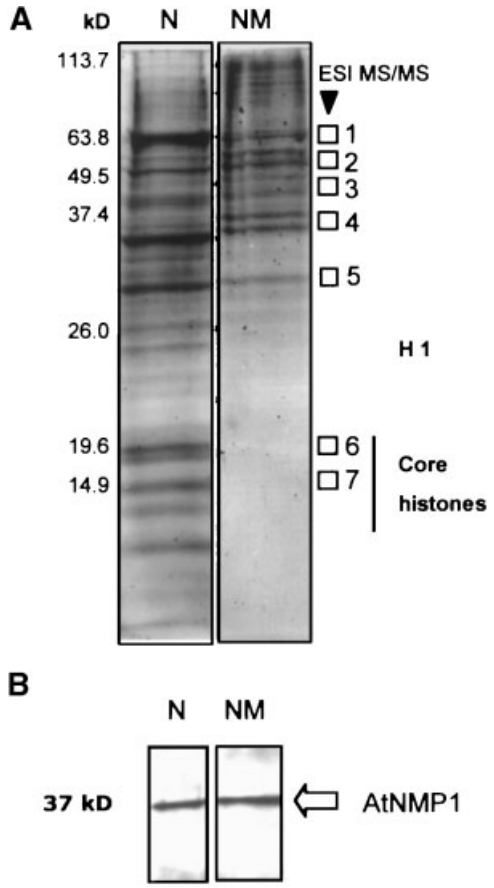

Fig. 3. **A**: Complexity of the Arabidopsis nuclear matrix compared to whole nuclei as resolved by 12% SDS–PAGE and stained with Coomassie Brilliant blue. N, nuclei, NM, nuclear matrix. The positions of the core histones and histone H1 in the nuclear fraction are indicated on the right. Squares with numbers indicate the location of the protein bands cut out for analysis by ESI MS/MS. The position of the molecular mass markers is indicated on the left. **B**: Immunoblot analysis with the anti-LeNMP1 antibody. N, nuclei; NM, nuclear matrix. A single band at 37 kDa, the predicted size of AtNMP1 (arrow), was detected in both fractions.

prediction algorithms (see "Materials and Methods"). Based on this analysis and the functional annotation of the polypeptides, the identified proteins were sorted into five groups: Proteins predicted to reside in the nucleoplasm, the nucleolus, the cytoplasm, proteins of unclear localization, and the proteins predicted to be located in other subcellular compartments (chloroplasts or mitochondria).

A protein was defined as nuclear if it contained a sequence experimentally verified as NLS or scored positive for nuclear localization by PSORT and Protcomp, or had been annotated as the Arabidopsis homologue of a nuclear protein. Four nuclear, non-nucleolar proteins were identified. Besides histone H2B, presumably present as a not-extracted remnant of the chromatin fraction, three novel proteins with unknown or putative functions were identified (Tables I and II). Sixteen proteins were identified that were predicted to have a nucleolar function. The nucleolar proteins were consistently identified with highest confidence based on Mascot Mowse scores and numbers of peptides, indicating their relative high abundance in the nuclear matrix fraction.

Many of the identified nucleolar proteins are homologues of proteins associated with snoRNP (small nucleolar ribonucleoprotein) complexes, such as the U3 snRNP protein IMP4, members of the Nop1/fibrillarin group, and a group of proteins homologous to Nop58p and Nop56p [Pih et al., 2000; Brown et al., 2003]. Two members of the Nop56/Nop58 family have previously been shown to be Matrix-attachment-region (MAR)-binding proteins forming part of the nuclear matrix in pea [Hatton and Gray, 1999]. Fibrillarin functions as an essential protein required for rRNA methylation, pre-rRNA cleavages and ribosome assembly [Venema and Tollervey, 1999; Fatica and Tollervey, 2002; Brown et al., 2003]. Nop56p and Nop58p form a core complex with Nop1p/fibrillarin, which is able to interact with small ribonucleolar RNAs within the context of C/D box snoRNPs [reviewed in Filipowicz and Pogacic, 2000; Brown et al., 2003]. IMP4 is involved in ribosomal RNA processing and was found in *Arabidopsis* both in the nucleoli and the associated Cajal bodies [Brown et al., 2003].

In addition to these proteins, a group of nucleolar proteins engaged in other functions has been identified. They include nucleolin, a ubiquitous MAR-binding nucleolar protein [Martin et al., 1992; Dickinson and Kohwi-Shigematsu, 1995]. This finding confirms molecularly previous reports by immunocytochemistry of nucleolin in the plant (onion) nucleolar matrix [Minguez and Moreno Diaz de la Espina, 1996].

Other putative nucleolar proteins included the ribosomal proteins L7, L5, and L18 [Fatica and Tollervey, 2002] and a protein highly homologous to the maize nucleolar HD2-p39-type histone deacetylase [Lusser et al., 1997]. In addition, an unknown protein was detected (AAM61154), which has a 41% amino acid identity (55% similarity) to the human nucleolar and coiled-body phosphoprotein 130

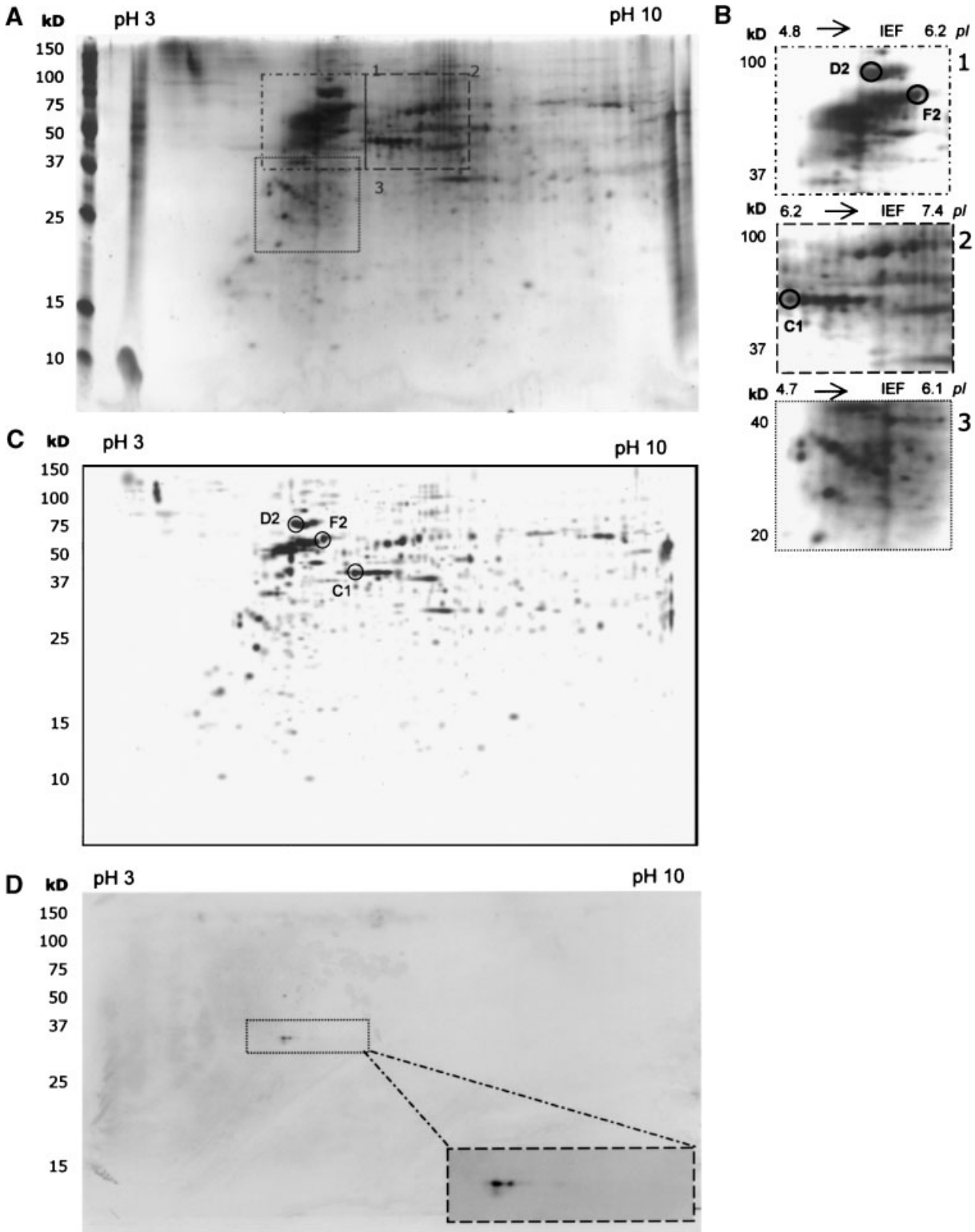

Fig. 4. Two-dimensional resolution of the Arabidopsis nuclear matrix, stained with SyproRuby, showing the original 2D gel (**A**), with insets (**B**) depicting three selected regions, which include the majority of protein spots. The numbered circles correspond to the polypeptides cored for the MALDI–TOF analysis (Table I). **C**: represents the image of the 2D gel shown in (A) generated by PDQuest (BioRad, Hercules, CA) after Gaussian analysis to remove background and enhance to protein spots of the lower abundance. **D**: 2D-immunoblot with the anti-LeNMP1 antibody. Inset shows the magnified region after chemiluminescent detection.

TABLE I. Proteins Identified After 2D Page and MALDI–TOF MS

Spot ID (MALDI–TOF)[a]	Functional classification[b]	Arabidopsis identity	Z score (profound); % coverage (MALDI)	Accession no.	Size of protein (kDa/aa)	Calculated pI (Expasy)	Protein localization[c] (NLS/ProtComp/ PSORT)	Other homologies [BLAST]/comments
Nucleus								
D2[d]	C7	Putative protein	0.66; 8%	NP_199663	75.5/671	5.9	–/N/N	11% Amino acid identity, 43% similarity to unknown protein IT1 [*Homo sapiens*] (AAB97010.11); 18% identity, 43% similarity to hypothetical protein MGC4701 [*Homo sapiens*] (NP_078787.1)
F2[d]	C7	Putative athila retroelement ORF1 protein	0.10; 14%	NP_178680	64.5/550	5.7	–/N/N	
Cytoplasm								
C1	C6	*S*-adenosylmethionine synthetase 3	0.05; 25%	Q96553	43/390	5.5	–/C/PX	
Localization uncertain								
D2[d]	C4	Heat-shock protein (At-hsc70-3)	0.66; 12%	NP_187555	71.1/694	4.9	–/N/PX	dnaK-type molecular chaperone hsc70.1 [*Arabidopsis thaliana*]
F2[d]	C7	Hypothetical protein	0.10; 14%	NP_172416	65.1/570	5.6	–/PX/M	36% Amino acid identity, 36% similarity to haploid germ cell-specific nuclear protein kinase [*Mus musculus*] (AF289866.1)

[a]Symbol designates an identifier of a protein spot from 2D-PAGE, analyzed by MALDI–TOF MS.
[b]Functional classification based on database annotation: C1—RNA modification and nucleic acid binding; C2—nucleotide binding; C3—ribosomal components; C4—chaperones; C5—elongation factors; C6—other; C7—unknown/novel proteins.
[c]Protein prediction: columbia predict NLS online/localization by ProtComp (Softberry Co.)/localization by PSORT v. 6.4. Symbols used: +, NLS detected (Columbia Predict NLS Online); –, NLS not detected; /N, localization in nucleus; C, cytoplasm; CN, localization in both cytoplasm and nucleus; M, mitochondrion; CH, chloroplast; PX, peroxisome; PM, plasma membrane; ER, endoplasmic reticulum; kDa, kiloDalton; aa, amino acid.
[d]Spots D2 and F2 were both found to contain two proteins, identified by MALDI–TOF MS.

TABLE II. Proteins Detected After 1D SDS–PAGE And ESI MS/MS

Obs. MM range (kDa)[a]	Functional classification[b]	Arabidopsis identity	Peptides	Total Mowse score (Mascot)/ Sonar score	Accession no.	Size of protein (kDa/aa)	Calculated pI (Expasy)	Protein localization[c]; NLS/ProtComp/ PSORT	Other homologies [BLAST]/comments
Nucleus									
20–22	C1	Histone H2B	LVLPGELAK QVHPDGISSK AMGIMNSFINDIFEK	124	CAA69025	16.3/145	10.9	+/N/N	
32–36	C7	K1G2.17~unknown protein	ATVISTPR	31	BAA95721	31.6/285	5.4	–/N/N	
Nucleolus									
56	C1	Putative SAR DNA binding protein	VVQLTAFHPFESALDALNQVNAVS EGVMTDELR IDCFADGATTAFGEK CPSSTLQILGAEK YGLIFHSSFIGR VREWYSWHFPELVK SFLELNLPK FSLGLAEPK IVNDNYLYAR IPCQSNEFVLELLR MSDIAPNLAALIGEMVGAR ASMGSDLSPLDLINVQTFAQK	346 Sonar 3.7×10^{-18}	NP_176007.1	58.8/522	8.7	+/N/N	58% Identity, 76% similarity to human nucleolar protein 5A/Nop56p (NP_006383.1)
50–55	C1	Putative SAR DNA-binding protein-1	TYNTAADSLLGETSAK MNTIAPNLTALVGELVGAR ELCDQVLSLSEYR FDNTSEALEAVAK IISDNILYAK QPGSTVQILGAEK SRMNTIAPNLTALVGELVGAR SQFTELISGLGDQDLAPMSLGLSHSLA SQFTELISGLGDQDLAPMSLGLSHSLAR	216	NP_187157	59.2/533	9.2	+/N/N	60% Identity, 76% similarity to nucleolar protein NOP5/NOP58 [*Xenopus laevis*] (AAH44082.1)
35–37	C1	Fibrillarin 1	GFGGGR VIVEPHR HAGVFIAK NLVPGEAVYNEK RISVQNEDGTKVEYR SVQNEDGTKVEYR VWNPFR LAAAILGGVDNIWIKPGAK KLQQEQFKPAEQVTLEPFER LQQEQFKPAEQVTLEPFER DHACVVGGYR TNVIPIIEDAR TNVIPIIEDARHPAK MLVGMVDVIFSDVAQPDQAR TGGHFVISIK ILALNASFFLK	111	AAG10103	32.8/308	10.1	+/N/PX	

TABLE II. (*Continued*)

Obs. MM range (kDa)[a]	Functional classification[b]	Arabidopsis identity	Peptides	Total Mowse score (Mascot)/ Sonar score	Accession no.	Size of protein (kDa/aa)	Calculated pI (Expasy)	Protein localization[c]; NLS/ProtComp/ PSORT	Other homologies [BLAST]/comments
32–36	C1	Fibrillarin 2 (AtFib2)	ILALNASYFLK NLVPGEAVYNEK LAAAILGGVDNIWIKPGAK LQQEQFKPAEQVTLEPFER VLYLGAASGTTVSHVSDLVGPEGCVYA-VEFSHR	239	NP_567724	35.5/320	10.0	+/N/N	
58	C1	Hypothetical protein At5g27120	LSNVEDLGNEFSTAK MNTIAPNLTALVGELVGAR SQLTELISGLGDQDLGPMSLGLSH-SLAR	265 Sonar 2.0×10^{-7}	O04658	58.9/439	9.2	–/N/N	SAR-like DNA-binding protein, 97% identity to NOP58-like protein F108 (*Arabidopsis thaliana*)
50–55	C1	Unknown putative protein	ELNTSLPDLEEIFSEFLNKR	41	AAM61154	36/330	5.7	+/N/N	41% Amino acid identity, 55% similarity to nucleolar and coiled-body phosphoprotein 130/ Nopp140 [*Homo sapiens*] (Q14978)
55–60	C1	NuM1 protein (nucleolin)	ADVENFFKEAGEVVDVR KAASSSDESSDDSSSDDEPAPK EPEDDIDTK TLFAANLSFNIER GFDASLSEDDIKNTLR ALELNGSDMGGGFYLVVDEPRPR GFGHVEFASSEEAQK DVIAAVQK	212	NP_175322	58.8/557	5.1	+/N/N	
32–36	C1	Putative U3 small nucleolar ribonucleoprotein protein	GVPDGLIISHLPFGPTAYFGLLNVVTR	59	NP_176564	32.6/294	9.3	–/N/PX	
29–33	C3	Ribosomal protein L7	ILGIEDLVNEIAR GCTIIEGNPVPLTDNNIIEQALGEHK	120	NP_178190	27.4/247	9.7	+/C/N	
18–22	C3	Putative 60S ribosomal protein L18	APLGQNTVLLR	58	AAA69928	20.9.187	10.9	–/C/C	
32–36	C3	Putative ribosomal protein L5	FTNKDIVAQIVSASIAGDIV	52	NP_566767	33.4/301	9.3	–/C/N	
28	C6	Putative histone deacetylase	SGKPVTVTPEEGILIHVSQASLGECK	51	NP_566872	26.6/245	5.1	–/N/N	Similar to the nucleolar HD2-p39-type deacetylase [*Zea mays*]
Cytoplasm									
44–49	C6	Putative s-adenosylmethionine synthetase	SGAYIVR	574	NP_188365	43.2/393	5.5	–/CN/C	

TABLE II. (*Continued*)

Obs. MM range (kDa)[a]	Functional classification[b]	Arabidopsis identity	Peptides	Total Mowse score (Mascot)/ Sonar score	Accession no.	Size of protein (kDa/aa)	Calculated pI (Expasy)	Protein localization[c]; NLS/ProtComp/ PSORT	Other homologies [BLAST]/comments
			ATIDYEKIVR SIVASGLAR ANVDYEQIVR IPDKEILEIVK FVIGGPHGDAGLTGR TNMVMVFGEITTK ESFDFRPGMISINLDLK TQVTIEYINESGAMVPVR KIIIDTYGGWGAHGGGAFSGK ESFDFRPGMISINLDLKR TAAYGHFGRDDADFTWEVVKPLK RVIVQVSYAIGVPEPLSVFVDSYGTGK ALVQVSYAIGVPEPLSVFVDTYGT-GLIPDKEILK					
50–55	C6	Tubulin beta-7 chain	MASTFIGNSTSIQEMFR GHYTEGAELIDSVLDVVR	100	NP_180515	50.5/449	4.7	–/C/C	
50–55	C6	Tubulin beta-9 chain	MASTFIGNSTSIQEMFR SGPFGQIFRPDNFVFGQSGAGNNWA	88	NP_193821	49.8/444	4.6	–/C/C	
55–60	C6	Tubulin beta-4 chain	GHYTEGAELIDSVLDVVRK SGPFGQIFRPDNFVFGQSGAGNNWAK	83	S68122	49.8/444	4.7	–/C/C	
55–60	C6	Tubulin beta-8 chain	GHYTEGAELIDSVLDVVRK SGPYGQIFRPDNFVFGQSGAGNNWAK	75	JQ1592	50.5/449	4.7	–/C/C	
50–55	C6	Tubulin alpha-6 chain	AVFVDLEPTVIDEVR	75	NP_193232	50/450	4.9	–/C/C	
55–60	C4	Heat shock dnaJ protein homologue atj3	EGMGGGGGGHDPF-DIFSSFFGGGPFGGNTSR	51	S71199	46.4/420	5.6	–/ER/C	
29–33	C6	Coatomer-like protein, epsilon subunit	VMQQIDEDHTLTQLASAWLN-LAVGGSK IQEAYLIFQDFSEKYPMTSLILNGK	64	AAM65018	32.1/289	5.3	–/C/C	
55–60	C1	F12M16.28	IEKEKAMEQENK	47	AAF69540	121/1096	9.2	–/PM/PM	ABC-family transporter protein (ATP-binding domain)
			MSVDRRNWLK TQGSIGK RNCMPCCEGFFCPRGLTCMIR CRLPADLSK						
50–55	C6	Polypeptide chain-binding protein homologue	LNVARIINEPTAAAIAYGLDK	Sonar 0.28	AAA92743	53.9/486	4.7	–/ER/C	[*Zea mays*] homologue
Localization uncertain									
50–55	C5	At1g07930/T6D22_3 putative translation elongation factor eEF-1	MTPTKPMVVETFSEYPPLGR	88	AAL57653	49.9/449	9.1	–/N/C	
			VETGMIKPGMVVTFAPTGLTTE						
40–45	C7	Unknown protein	GGALLNIITEPGFHLK	208	AAM65678	38.4/356	5.6	–/PM/ER	55% Identity and 75% similarity to hypothetical protein MGC27952 [*Mus musculus*] (NP_705820.1)

TABLE II. (*Continued*)

Obs. MM range (kDa)[a]	Functional classification[b]	Arabidopsis identity	Peptides	Total Mowse score (Mascot)/ Sonar score	Accession no.	Size of protein (kDa/aa)	Calculated pI (Expasy)	Protein localization[c]; NLS/ProtComp/ PSORT	Other homologies [BLAST]/comments
			LPFITNYEPVQVTLQTDQVR YAPGIEILSVR IFFGDKVPNMVLDQR						
44–49	C7	Expressed protein	TTAVSLPR	40	NP_566713	22/203	6.1	–/EX/PM	
44–49	C5	Putative protein	NIAAPLDPAAFSADAVVQIYHDNAG-DLELELVAK	36	NP_568534.1	45.6/411	5.5	–/CH/N	32% Amino acid identity to basic leucine zipper and W2 domains 2 [*Mus musculus*] (AAH13060); elongation initiation factor 5C [*Drosophila melanogaster*]
Other cellular compartments									
44–49	C5	Putative chloroplast translation elongation factor EF-Tu precursor	ILDEALAGDNVGLLLR	194	AAN31832	52.8/476	5.8	–/CH/CH	
			QTELPFLLAVEDVFSITGR QVGVPDMVVFLNKEDQVDDAELLEL-VELEVR						
29–33	C2	Adenylate translocator	LLIQNQDEMIK	183 Sonar 5.8×10^{-3}	NP_187470	42.3/381	9.8	–/M/M	
			YFPTQALNFAFK GFTNFALDFLMGGVSAAVSK AVAGAGVLSGYDKLQLIVFGK						
29–33	C2	ADP, ATP carrier protein adenosine nucleotide translocator	LLIQNQDEMLK	132 Sonar 0.41	S29852	42.7/385	9.8	–/M/PX	
			YFPTQALNFAFK GFTNFAIDFMMGGVSAAVSK						

[a]Obs MM, observed molecular mass range of proteins excised from 1D SDS–PAGE (kDa).
[b]Functional classification based on database annotation: C1—RNA modification and nucleic acid binding; C2—nucleotide binding; C3—ribosomal components; C4—chaperones; C5—elongation factors; C6—other; C7—unknown/novel proteins.
[c]Protein prediction: Columbia Predict NLS Online/localization by ProtComp (Softberry Co.)/Localization by PSORT v. 6.4. Symbols used: +, NLS detected (Columbia Predict NLS Online); –, NLS not detected; /N, localization in nucleus; C, cytoplasm; CN, localization in both cytoplasm and nucleus; M, mitochondrion; CH, chloroplast; PX, peroxisome; PM, plasma membrane; ER, endoplasmic reticulum; kDa, kiloDalton; aa, amino acid.

(Nopp140). Nopp140 functions in nucleologenesis, and may play a role in the maintenance of the dense fibrillar component in the nucleolus [Pai et al., 1995; Chen et al., 1999].

The third general class of proteins is composed of those predicted to be cytoplasmic. It is possible that some proteins of this class represent cytoplasmic contaminants, however, their true subcellular location will have to be determined experimentally. The major proteins in this group were identified several times, both by ESI MS/MS and by MALDI–TOF, and found to have very high Mascot Mowse scores, indicating that they are abundant proteins in the fraction.

The most prominent proteins of this group were two putative *S*-adenosylmethionine synthases (SAM synthase). SAM synthase catalyses the conversion of ATP and L-methionine into *S*-adenosyl-L-methionie (SAM). SAM functions as a methyl group donor for various transmethylation reactions and as a cofactor in metabolic reactions [Tabor and Tabor, 1984].

In addition, a number of α- and β-tubulins were identified. It cannot be ruled out that the tubulin components co-purified as cytoplasmic inclusions, especially since in animal apoptotic cells they have also been found to co-isolate with nuclear fractions, likely as a result of the tubulin network collapsing towards the nuclear surface [Gerner et al., 2002]. Other proteins in this group were F12M16.28, homologous to an ABC-transporter protein and a homologue of the co-chaperone DnaJ (S71199).

The fourth class includes the proteins with unclear predicted localization. The proteins of this group included a homologue of translation elongation factor eEF-1 and the heat shock protein At-hsc70-3, which is predicted to be localized in the cytoplasm, but also contains consensus sequences for nuclear targeting [Lin et al., 2001]. Among other proteins found in the Arabidopsis nuclear matrix was an unknown protein AAM65678, which shares 55% identity and 75% similarity on the amino acid level with the mouse hypothetical protein MGC27952 (NP_705820.1). Another identified protein was the putative protein NP_568534 with 32% amino acid identity to a mouse protein containing a basic leucine zipper and W2 domain 2 (locus AAH13060), a protein-protein interaction domain found in several translation elongation factors.

Finally, chloroplast translation elongation factor EF-Tu, an adenylate translocator (NP_187470), and an ADP, ATP carrier protein (S29852) were identified. They are predicted to be located in the chloroplast or mitochondria, and therefore most likely represent contamination of the nuclear matrix preparation with these organelles.

Figure 5 shows the predicted subcellular localization and functional annotation of all identified proteins.

Coiled-Coil Domains in Arabidopsis Nuclear Matrix Proteins With Unknown Functions

Proteins with unknown or unclear function were searched for coiled-coil domains, which are found in filamentous nuclear proteins, such as lamins or NuMA [Lydersen and Petijohn, 1980]. We found four proteins containing coil-coiled motifs (AAM61154, BAA95721, NP_176007, and NP_566231), but only AAM61154 has a coil-coiled motif of sufficient length (amino acids 31–212, encompassing two-thirds of the protein) to predict a possible structural function.

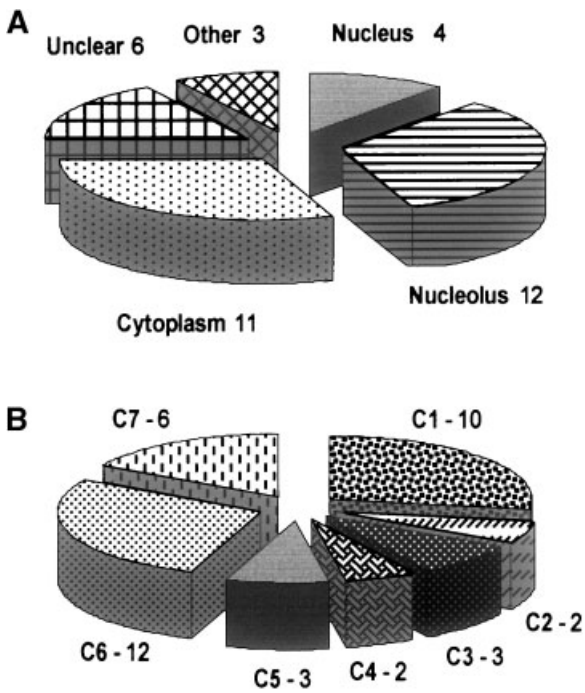

Fig. 5. **A**: Predicted subcellular localization of the proteins identified in the Arabidopsis nuclear matrix. **B**: Functional classification of the proteins identified in the Arabidopsis nuclear matrix based on the database annotation: **C1**—RNA modification and nucleic acid binding; **C2**—nucleotide binding; **C3**—ribosomal components; **C4**—chaperones; **C5**—elongation factors; **C6**—other; **C7**—unknown/novel proteins.

DISCUSSION

This is the first ultrastructural analysis and identification of a number of proteins present in the nuclear matrix of Arabidopsis. A previous ultrastructural and 2D-PAGE investigation of a higher plant nuclear matrix [from onion—Yu and Moreno Diaz de la Espina, 1999] was based on salt extraction instead of LIS. The described nucleolar and internal nuclear matrices are structurally very comparable to what we found here, displaying a classic core filament, highly networked organization, with characteristically knobby protrusions decorating the filaments. This demonstrates that the essential elements of the nuclear matrix as previously described for animal nuclei [Berezney and Coffey, 1977; Brasch, 1982; Berezney, 1984; Mirkovitch et al., 1984] can be revealed by either high-salt or LIS extraction from higher plants too.

The analysis of proteins identified in the nuclear matrix fraction reveals a high enrichment of proteins associated with the nucleolus. It also demonstrates the preservation of essential nucleolar components, as shown previously by others [Nickerson et al., 1990; Minguez and Moreno Diaz de la Espina, 1996; Spiker and Thompson, 1996]. In particular, the members of the box C/D snoRNP family are well represented (no members of box H/ACA group of snoRNPs were detected). They include proteins responsible for ribosome biogenesis and the maturation of RNA, such as fibrillarin and nucleolin, which have been shown to shuttle rapidly between nucleolus and nucleoplasm [Chen and Huang, 2001] as well as a group of proteins homologous to yeast Nop58p and Nop56p [Brown et al., 2003], which had been previously identified as SAR-binding proteins in the pea nuclear matrix [Hatton and Gray, 1999].

Several of the identified proteins are directly or indirectly involved in nucleolar methylation reactions. The snoRNA-associated proteins direct 2′-*O*-ribose-methylation of small nucleolar RNAs (snoRNAs), and fibrillarin (yeast Nop1p homologue) has been proposed to function as an essential rRNA methylase in eukaryots, including *Arabidopsis* [Barneche et al., 2000; Pih et al., 2000]. Fibrillarin has been shown to associate in vivo with RNA and with U3 snoRNA-binding proteins, which were also identified here. The *Arabidopsis* AtFib1 and AtFib2 proteins found in this study were shown to function as homologs of yeast Nop1/fibrillarin and contain the putative AdoMet-dependent methylotransferase motifs [Niewmierzycka and Clarke, 1999; Barneche et al., 2000]. Although there is no evidence at present that the S-Adenosylmethionine used for nuclear methylation reactions is synthesized inside the nucleus, the abundant presence of SAM-synthase in our preparations, together with these nucleolar nucleic acid methylating proteins, encourages a reinvestigation of the subcellular localization of SAM-synthase by cell biological approaches.

Nucleolin constitutes one of the most abundant nucleolar proteins, and can represent as much as 10% of total nucleolar protein in animal systems [Ginisty et al., 1999]. Interestingly, it was found to interact not only with rRNA, a feature critical for its nucleolar localization [Ginisty et al., 1999] but also with many proteins, including U3 snoRNP [Ginisty et al., 1998], and ribosomal proteins found in this study. The multiple functions of nucleolin include the ability to bind the Matrix Attachment Regions (MARs), supporting its role within the formation of the nucleolar matrix [Martin et al., 1992; Martelli et al., 1995; Minguez and Moreno Diaz de la Espina, 1996].

The putative histone deacetylase identified here is highly homologous to the maize nucleolar HD2-p39-type histone deacetylase [Lusser et al., 1997]. Nucleolar histone deacetylases have been connected to the silencing of ribosomal DNA transcription by RNA polymerase I in the nucleolus [Hirschler-Laszkiewicz et al., 2001; Bjerling et al., 2002]. Connections between histone acetylation, regulation of Pol II transcription, and the nuclear matrix have been made previously in animal systems [Davie, 1996; Westendorf et al., 2002], and finding a nucleolar histone modifying protein in a plant nuclear matrix now adds to the list of nuclear activities associated with this fraction.

Two putative chaperone proteins were identified in this study, the Arabidopsis HSP/HSC70 homolog At-hsc70-3, and the Arabidopsis homolog of DNAj (atj3), a co-chaperone of the yeast HSP/HSC70 homolog DnaK. Brine shrimp (*Artemia franciscana*) HSP70 has been shown to associate with the small heat shock protein p26 and with nuclear lamins within the context of the nuclear matrix, presumably preventing protein unfolding upon cellular stress [Willsie and Clegg, 2002]. Similar results were also obtained in other experimental animal and

human systems [Pouchelet et al., 1983; Gerner et al., 1999; Gerner et al., 2002]. Interestingly, it has previously been shown that the members of the mammalian HSP/HSC70 family are able to bind RNA via their N-terminal ATP-binding domain, in a process dependent on the interaction with co-chaperones such as DnaJ [Zimmer et al., 2001]. It is tempting to speculate that this phenomenon extends to the nuclear matrix, or to the integral ribonucleoprotein complexes found therein, especially in the light of the proposed "RNA-chaperone" function of the HSC/HSP70 proteins [Zimmer et al., 2001].

Translation factors have been identified previously by proteomic approaches in the human nucleolus [Scherl et al., 2002] and in the human nuclear matrix [Holzmann et al., 2000]. Here, we have identified the Arabidopsis homolog of eukaryotic elongation factor 1 (eEF1), which was found in the human nucleolus [Scherl et al., 2002]. The identification of different elements of translation (translation factors, ribosomal subunits) in the nuclear matrix gains relevance from the recent demonstration of nuclear translation [Iborra et al., 2001] and the association of ribosome components with the sites of transcription and nascent RNP complexes [Brogna et al., 2002]. To our knowledge, this is the first report of a translation factor found associated with a nuclear compartment in plants.

The presented study demonstrates the applicability of the proteomic approach to the nuclear matrix of higher plants (*A. thaliana*). While not complete, it gives an insight into the most abundant protein components. On the other hand, the real number of proteins of nuclear matrix might be lower than estimated from the 2D analysis, since many spots may have resulted from posttranslational modifications, including phosphorylation, as suggested by the result of the 2D NMP1 immunoblotting experiment. While it is indicated in the literature that many proteins identified in this study are engaged in reciprocal interactions, forming large protein complexes (e.g., nucleolar proteins Nop56p/Nop58p and fibrillarin proteins, nucleolin and U3 snoRNP and the ribosomal components), it would be premature to attempt drawing any "interaction map" between these proteins. However, with a larger number of proteins identified, and investigated, for example, by reciprocal yeast two hybrid assays, drawing such a map should allow for the elucidation of the functional interactions between nuclear matrix proteins. Similarly, the analysis of the novel proteins identified here will aid in this purpose, especially when combined with immunogold electron microscopy of the isolated nuclear matrices once antibodies become available. These approaches should ultimately lead to an answer to the question whether the proteins of the operationally defined nuclear matrix are true in vivo interaction partners and which proteins are components of the observed filaments.

ACKNOWLEDGMENTS

We thank the Ohio State University Plant-Microbe Genomics Facility for financial support (proteomics seed grant), and David Mandich for excellent technical assistance with two-dimensional gel electrophoresis. We thank Dr. Kari Green-Church from the OSU Campus Chemical Instrument Center for excellent cooperation with mass spectrometric identification of proteins. This work was supported by a grant from the National Science Foundation (MCB-0079577) to Iris Meier.

REFERENCES

Altschul SF, Gish W, Miller W, Myers EW, Lipman DJ. 1990. Basic local alignment tool. J Mol Biol 215:403–410.

Andersen JS, Lyon CE, Fox AH, Leung AK, Lam YW, Steen H, Mann M, Lamond AI. 2002. Directed proteomic analysis of the human nucleolus. Curr Biol 12:1–11.

Barneche F, Steinmetz F, Echeverria M. 2000. Fibrillarin genes encode both a conserved nucleolar protein and a novel small nucleolar RNA involved in ribosomal RNA methylation in *Arabidopsis thaliana*. J Biol Chem 275: 27212–27220.

Belgrader P, Siegel AJ, Berezney R. 1991. A comprehensive study on the isolation and characterization of the HeLa S3 nuclear matrix. J Cell Sci 98:281–291.

Berezney R. 1984. Organization and functions of the nuclear matrix. In: Hnilica LS, editor. Chromosomal nonhistone proteins. Vol. IV. Boca Raton, FL: CRC Press. pp 119–180.

Berezney R, Coffey DS. 1974. Identification of a nuclear protein matrix. Biochem Biophys Res Commun 60:1410–1417.

Berezney R, Coffey DS. 1977. Nuclear matrix. Isolation and characterization of a framework structure from rat liver nuclei. J Cell Biol 73:616–637.

Berezney R, Mortillaro MJ, Ma H, Wei X, Samarabandu J. 1995. The nuclear matrix: A structural milieu for genomic function. Int Rev Cytol 162A:1–65.

Bjerling P, Silverstein RA, Thon G, Caudy A, Grewal S, Ekwall K. 2002. Functional divergence between histone deacetylases in fission yeast by distinct cellular localization and in vivo specificity. Mol Cell Biol 22:2170–2181.

Brasch K. 1982. Fine structure and localization of the nuclear matrix in situ. Exp Cell Res 140:161–171.

Brogna S, Sato TA, Rosbash M. 2002. Ribosome components are associated with sites of transcription. Mol Cell 10:93–104.

Brown JW, Echeverria M, Qu LH. 2003. Plant snoRNAs: Functional evolution and new modes of gene expression. Trends Plant Sci 8:42–49.

Chen D, Huang S. 2001. Nucleolar components involved in ribosome biogenesis cycle between the nucleolus and nucleoplasm in interphase cells. J Cell Biol 153:169–176.

Chen HK, Pai CY, Huang JY, Yeh NH. 1999. Human Nopp140, which interacts with RNA polymerase I: Implications for rRNA gene transcription and nucleolar structural organization. Mol Cell Biol 19:8536–8546.

Chi-Ham CL, Keaton MA, Cannon GC, And Heinhorst S. 2002. The DNA-compacting protein DCP68 from soybean chloroplasts is ferrodoxin:sulfite reductase and co-localizes with the organellar nucleoid. Plant Mol Biol 49: 621–631.

Cokol M, Nair R, Rost B. 2000. Finding nuclear localization signals. EMBO Rep 1:411–415.

Davie JR. 1996. Histone modifications, chromatin structure, and the nuclear matrix. J Cell Biochem 62:149–157.

Dickinson LA, Kohwi-Shigematsu T. 1995. Nucleolin is a matrix attachment region DNA-binding protein that specifically recognizes a region with high base-unpairing potential. Mol Cell Biol 15:456–465.

Dreger M, Bengtsson L, Schoneberg T, Otto H, Hucho F. 2001. Nuclear envelope proteomics: Novel integral membrane proteins of the inner nuclear membrane. Proc Natl Acad Sci USA 98:11943–11948.

Fatica A, Tollervey D. 2002. Making ribosomes. Curr Opin Cell Biol 14:313–318.

Fawcet DW. 1966. An atlas of fine structure: The cell, its organelles and inclusions. Philadelphia: W.B. Saunders Co.

Filipowicz W, Pogacic V. 2000. Biogenesis of small nucleolar ribonucleoproteins. Curr Opin Cell Biol 14:319–327.

Gerner C, Holzmann K, Grimm R, Sauermann G. 1998. Similarity between nuclear matrix proteins of various cells revealed by an improved isolation method. J Cell Biochem 71:363–374.

Gerner C, Holzmann K, Meissner M, Goetzmann J, Grimm R, Sauermann G. 1999. Reassembling proteins and chaperones in human nuclear matrix protein fractions. J Cell Biochem 74:145–151.

Gerner C, Gotzmann J, Froehwein U, Schamberger C, Ellinger A, Sauermann G. 2002. Proteome analysis of nuclear matrix proteins during apoptotic chromatin condensation. Cell Death Differentiation 9:671–681.

Gindullis F, Meier I. 1999. Matrix attachment region binding protein MFP1 is located in discrete domains at the nuclear envelope. Plant Cell 11:1117–1128.

Ginisty H, Amalric F, Bouvet P. 1998. Nucleolin functions in the first step of ribosomal RNA processing. EMBO J 17:1476–1486.

Ginisty H, Sicard H, Roger B, Bouvet P. 1999. Structure and functions of nucleolin. J Cell Sci 112:761–772.

Hall G, Jr., Allen GC, Loer DS, Thompson WF, Spiker S. 1991. Nuclear scaffolds and scaffold-attachment regions in higher plants. Proc Natl Acad Sci USA 88:9320–9324.

Hancock R. 2000. A new look at the nuclear matrix. Chromosoma 109:219–225.

Hatton D, Gray JC. 1999. Two MAR DNA-binding proteins of the pea nuclear matrix identify a new class of DNA-binding proteins. Plant J 18:417–429.

Hirschler-Laszkiewicz I, Cavanaugh A, Hu Q, Catania J, Avantaggiati ML, Rothblum LI. 2001. The role of acetylation in rDNA transcription. Nucleic Acids Res 29:4114–4124.

Holzmann K, Gerner C, Poltl A, Schafer R, Obrist P, Ensinger C, Grimm R, Sauermann G. 2000. A human common nuclear matrix protein homologous to eukaryotic translation initiation factor 4A. Biochem Biophys Res Commun 267:339–344.

Iborra FJ, Jackson DA, Cook PR. 2001. Coupled transcription and translation within nuclei of mammalian cells. Science 293:1139–1142.

Lin BL, Wang JS, Liu HC, Chen RW, Meyer Y, Barakat A, Delseny M. 2001. Genomic analysis of the Hsp70 superfamily in *Arabidopsis thaliana*. Cell Stress Chaperones 6:201–208.

Lothstein L, Arensdorf HP, Chung S-Y, Walker BW, Wooley JC, LeSturgeon WM. 1985. General organization of protein in HeLa 40S nuclear ribonucleoprotein particles. J Cell Biol 100:1570–1581.

Lusser A, Brosch G, Loidl A, Haas H, Loidl P. 1997. Identification of maize histone deacetylase HD2 as an acidic nucleolar phosphoprotein. Science 277:88–91.

Lydersen BK, Petijohn DE. 1980. Human-specific nuclear protein that associates with the polar region of the mitotic apparatus: Distribution in a human/hamster hybrid cells. Cell 22:489–499.

Martelli AM, Manzoli L, Rubbini S, Billi AM, Bareggi R, Cocco L. 1995. The protein composition of Friend cell nuclear matrix stabilized by various treatments. Different recovery of nucleolar proteins B23 and C23 and nuclear lamins. Biol Cell 83:15–22.

Martelli AM, Falcieri E, Zweyer M, Bortul R, Tabellini G, Cappellini A, Cocco L, Manzoli L. 2002. The controversial nuclear matrix: A balanced point of view. Histol Histopathol 17:1193–1205.

Martin M, Garcia-Fernandez LF, Diaz de la Espina SM, Noaillac-Depeyre J, Gas N, Javier Medina F. 1992. Identification and localization of a nucleolin homologue in onion nucleoli. Exp Cell Res 199:74–84.

Minguez A, Moreno Diaz de la Espina S. 1996. In situ localization of nucleolin in the plant nucleolar matrix. Exp Cell Res 222:171–178.

Mirkovitch J, Mirault ME, Laemmli UK. 1984. Organization of the higher-order chromatin loop: Specific DNA attachment sites on nuclear scaffold. Cell 39:223–232.

Nakai K, Kanehisa M. 1992. A knowledge base for predicting protein localization sites in eukaryotic cells. Genomics 14:897–911.

Nickerson JA. 2001. Experimental observations of a nuclear matrix. J Cell Sci 114:463–474.

Nickerson JA, Krockmalnic G, He DC, Penman S. 1990. Immunolocalization in three dimensions: Immunogold staining of cytoskeletal and nuclear matrix proteins in resinless electron microscopy sections. Proc Natl Acad Sci USA 87:2259–2263.

Nickerson JA, Krockmalnic G, Wan KM, Penman S. 1997. The nuclear matrix revealed by eluting chromatin from a cross-linked nucleus. Proc Natl Acad Sci USA 94:4446–4450.

Niewmierzycka A, Clarke S. 1999. *S*-adenosylmethionine-dependent methylation in *Saccharomyces cerevisiae*. Identification of a novel protein argininemethyltransferase. J Biol Chem 274:814–824.

Pai CY, Chen HK, Shen HL, Yeh NH. 1995. Cell-cycle-dependent alterations of a highly phosphorylated nucleolar protein p130 are associated with nucleologenesis. J Cell Sci 108:1911–1920.

Pederson T. 1998. Thinking about a nuclear matrix. J Mol Biol 277:147–159.

Pederson T. 2000. Half a century of "the nuclear matrix." Mol Biol Cell 11:799–805.

Penman S. 1995. Rethinking cell structure. Proc Natl Acad Sci USA 92:525–527.

Pih KT, Yi MJ, Liang YS, Shin BJ, Cho MJ, Hwang I, Son D. 2000. Molecular cloning and targeting of a fibrillarin homolog from arabidopsis. Plant Phys 123:51–58.

Pouchelet M, St-Pierre E, Bibor-Hardy V, Simard R. 1983. Localization of the 70,000 dalton heat-induced protein in the nuclear matrix of BHK cells. Exp Cell Res 149:451–459.

Rose A, Gindullis F, Meier I. 2003. A novel alpha-helical protein, specific to and highly conserved in plants, is associated with the nuclear matrix fraction. J Exp Botany 54:1–9.

Scherl A, Couté Y, Déon C, Callé A, Kindbieter K, Sanchez J-C, Greco A, Hochstrasser D, Diaz J-J. 2002. Functional proteomic analysis of human nucleolus. Mol Biol Cell 13:4100–4109.

Smetana K, Steele WJ, Busch H. 1966. A ribonucleoprotein network. Exp Cell Res 31:198–201.

Spiker S, Thompson WT. 1996. Nuclear matrix attachment regions and transgene expression in plants. Plant Physiol 110:15–21.

Tabor CW, Tabor H. 1984. Methionine adenosyltransferase (*S*-adenosylmethionine synthase) and *S*-adenosylmethione decarboxylase. Adv Enzymol 56:251–282.

Tan J-H, Wooley JC, LeSturgeon WM. 2000. Nuclear matrix-like filaments and fibrogranular complexes form through the rearrangement of specific nuclear ribonucleoproteins. Mol Biol Cell 11:1547–1554.

van Holde KE. 1989. Chromatin. New York: Springer.

Venema J, Tollervey D. 1999. Ribosome synthesis in *Saccharomyces cerevisiae*. Annu Rev Genet 33:261–311.

Washburn MP, Wolters D, Yates JR III. 2001. Large-scale analysis of the yeast proteome by multidimensional protein identification technology. Nat Biotechnol 19:242–247.

Westendorf JJ, Zaidi SK, Cascino JE, Kahler R, van Wijnen AJ, Lian JB, Yoshida M, Stein GS, Li X. 2002. Runx2 (Cbfa1, AML-3) interacts with histone deacetylase 6 and represses the p21(CIP1/WAF1) promoter. Mol Cell Biol 22:7982–7992.

Willsie JK, Clegg JS. 2002. Small heat shock protein p26 associates with nuclear lamins and HSP70 in nuclei and nuclear matrix fractions from stressed cells. J Cell Biochem 84:601–614.

Yu W, Moreno Diaz de la Espina S. 1999. The plant nucleoskeleton: Ultrastructural organization and identification of NuMA homologues in the nuclear matrix and mitotic spindle of plant cells. Exp Cell Res 246:516–526.

Zimmer C, von Gabain A, Henics T. 2001. Analysis of sequence-specific binding of RNA to Hsp70 and its various homologs indicates the involvement of N- and C-terminal interactions. RNA 7:1628–1637.